Effects of an anisotropic relaxation time on the electron-electron scattering resistivity in K and Cu

1989 J. Phys.: Condens. Matter 1 3621

(http://iopscience.iop.org/0953-8984/1/23/007)

J. Phys.: Condens. Matter 1 (1989) 3621–3643. Printed in the UK

Effects of an anisotropic relaxation time on the electron–electron scattering resistivity in K and Cu

J Sprengel†§, G Thummes‡ and J Appel†

† Institut für Theoretische Physik, Universität Hamburg, D-2000 Hamburg 36, Federal Republic of Germany

‡ Institut für Angewandte Physik, Universität Hamburg, D-2000 Hamburg 36, Federal Republic of Germany

Received 15 July 1988, in final form 8 September 1988

Abstract. The contribution of normal electron–electron scattering to the electrical resistivity of K and Cu in the presence of an anisotropic relaxation time is calculated using the relaxation time approximation (RTA) and also, for the first time, using the formally exact variational method. As sources of anisotropic scattering we consider (i) electron–dislocation scattering according to a model of Kaveh and Wiser for potassium, and (ii) a high longitudinal magnetic field $\boldsymbol{B}$ applied to a copper single crystal. It is found that, as compared with the variational method, the RTA overestimates the increase of the electron–electron scattering resistivity $\rho_{ee} = A_{ee}T^2$ with anisotropy. The calculated enhancement of A_{ee} in copper by a magnetic field depends sensitively on the crystallographic orientation. Comparison with the experimental coefficients A_{ee} for $\boldsymbol{B} \parallel \langle 111 \rangle$ yields an Umklapp fraction of $\Delta \simeq 0.04$–0.06 for electron–electron scattering in Cu, which is smaller than $\Delta \simeq 0.28$ as previously calculated by Black. The dislocation model cannot account quantitatively for the large variation in the experimental A_{ee} in potassium.

1. Introduction

During the last decade the development of high-resolution experimental techniques at low temperatures has made possible the measurement of the electron–electron scattering (EES) contribution $\rho_{ee}(T) = A_{ee}T^2$ to the electrical resistivity $\rho(T)$ of simple metals. For recent reviews see Schroeder (1982), Kaveh and Wiser (1984), Wiser (1984), and van Vucht *et al* (1985). The most striking observation from the experimental results is that the T^2 coefficient A_{ee} is not the same for all samples of the same metal but exhibits a considerable sample dependence, in particular for K and Cu.

Kaveh and Wiser (KW) (1980, 1982, 1983) have shown that the variation in A_{ee} may be explained by deviations from Matthiessen's rule (DMR). This deviation, following an idea of Peierls (1955), can be related to the indirect contribution of normal electron–electron scattering (NEES) to $\rho_{ee}(T)$ in the presence of an anisotropy in the electron relaxation time $\tau(\boldsymbol{K})$ on the Fermi surface (FS). At the low temperatures where $\rho_{ee}(T)$ can be observed, $\tau(\boldsymbol{K})$ is determined by the scattering from static lattice defects, predominantly from impurities and dislocations. In contrast to Umklapp electron–electron scattering (UEES), NEES itself does not contribute to the resistivity because of momentum conservation which implies current conservation in the case of a spherical FS. However,

§ Present address: Institut für Angewandte Physik, Universität Hamburg, D-2000 Hamburg 36, Federal Republic of Germany.

0953-8984/89/233621 + 23 $02.50

NEES in the presence of an anisotropic $\tau(\boldsymbol{K})$ will redistribute the conduction electrons by scattering them into regions of small $\tau(\boldsymbol{K})$ and thus will reduce the current. KW assume dislocation scattering to be the source of anisotropy in $\tau(\boldsymbol{K})$ and derive an expression for the enhancement of A_{ee} by dislocations

$$A_{ee} = A_{ee}^{iso}\left[1 + SD\left(1 + \frac{\rho_{imp}}{\rho_{dis}}\right)^{-2}\right]. \tag{1.1}$$

Here ρ_{imp} and ρ_{dis} denote the contributions of (isotropic) impurity and (anisotropic) dislocation scattering to the residual resistivity $\rho_r \equiv \rho(T \rightarrow 0)$ of a metal sample. When the isotropic limit A_{ee}^{iso} and the 'sample dependence' SD (defined in equation (3.10)) are used as fitting parameters, then fairly good agreement is found with the experimental data for K and Cu (Steenwyck *et al* 1981, Zwart *et al* 1983, Thummes and Kötzler 1985).

Recently, Thummes and Kötzler (1985) have also observed a strong enhancement of A_{ee} by a high longitudinal magnetic field in single crystals of Cu. The enhancement is related qualitatively to a magnetic-field-induced anisotropy in $\tau(\boldsymbol{K})$.

Although the effect of anisotropy on the NEES contribution to A_{ee} is beyond doubt, the maximum possible value of A_{ee} in the anisotropic limit, and thus the sample dependence which can be caused by NEES, is still ambiguous. The calculations of KW leading to equation (1.1) are based on a 'generalised' relaxation time approximation (RTA) originally used by Callaway (1959) for the case of phonon scattering, the validity of which cannot be easily estimated.

In this work we present calculations of the variation of A_{ee} with the anisotropy in $\tau(\boldsymbol{K})$. We consider two anisotropy models which are introduced in § 2. These models are (i) dislocation-induced anisotropy according to KW (1980, 1982), and (ii) magnetic-field-induced anisotropy in $\tau(\boldsymbol{K})$ in a Cu single crystal as proposed by Thummes and Kötzler (1985). The calculations of A_{ee} (§ 3) are made by use of the RTA and, for the first time, also by use of the formally exact variational method (see for example Kohler 1948, and Ziman 1960), which allows conclusions about the validity of the RTA results.

The main results, discussed in § 4, are as follows: (i) the RTA overestimates the effect of anisotropy on A_{ee} for both models of $\tau(\boldsymbol{K})$; (ii) the dislocation model cannot account quantitatively for the experimentally observed strong sample dependence of A_{ee} in K; and (iii) a longitudinal magnetic field enhances A_{ee} in Cu to a maximum value which depends sensitively on the crystallographic orientation, that is, on the position of the necks on the FS with respect to the field. Comparison with the experimental data for Cu shows that the calculated effect on A_{ee} is lower than observed experimentally. The agreement with the experiment may be improved by using in the isotropic limit a smaller UEES contribution than that calculated by Black (1978) for Cu, or by taking a more refined FS model in the calculation of the transport averages of $\tau(\boldsymbol{K})$ as shown in Appendix 3.

2. Models of relaxation time anisotropy

2.1. Dislocation-induced anisotropy

Dislocations are expected to cause an anisotropic relaxation time $\tau_{dis}(\boldsymbol{K})$, see, e.g., Wiser (1984). First, this is due to the marked spatial anisotropy of a dislocation line, which scatters electrons moving perpendicular to it more strongly than those moving parallel. Second, the long-range strain fields surrounding the dislocation core give rise to a large number of small-angle scattering events, which effectively degrade the current

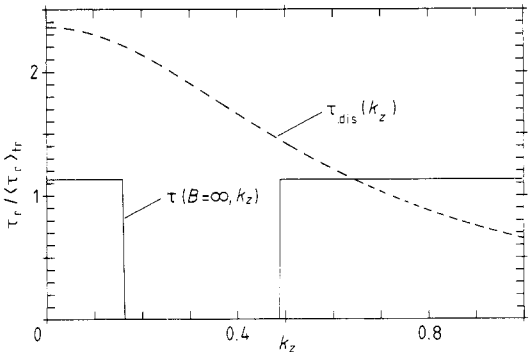

Figure 1. Models for an anisotropic relaxation time $\tau(K_z)$. Broken curve: dislocation scattering $\tau_{dis}(K_z)$ according to equation (2.1) with $\gamma/\beta = (\frac{7}{8})^{1/2}$ for K. Solid line: scattering in a high longitudinal magnetic field in a ⟨111⟩-Cu sample, according to equation (2.9). Both curves are normalised to the transport averages $\langle\tau_{dis}\rangle_{tr}$ and $\langle\tau(B, K_z)\rangle_{tr}$, respectively, as defined in equation (3.2*a*).

in those $\boldsymbol{K}$-regions where the FS has a strong curvature. This second mechanism, as first suggested by Dugdale and Basinski (1967), probably determines the anisotropic electron-dislocation scattering in the noble metals, where $\tau_{dis}(\boldsymbol{K})$ is much lower in the neck regions on the FS than in the nearly spherical belly regions (Bergmann *et al* 1981).

For dislocation-induced anisotropy we consider here the model of KW (1980, 1982), which they originally use to calculate the sample dependence of A_{ee} in potassium and later also apply to copper. Within this model, $\tau_{dis}^{-1}(\boldsymbol{K})$ depends only on the component K_z of the wavevector parallel to the electric field and is given by a lowest-order Legendre expansion:

$$\tau_{dis}^{-1}(\boldsymbol{K}) = \beta + \gamma P_2(K_z) \tag{2.1}$$

where β denotes the average value on the FS and $P_2(K_z)$ is the second Legendre polynomial. The function $\tau_{dis}(\boldsymbol{K})$ according to equation (2.1), with $\gamma/\beta = (\frac{7}{8})^{1/2}$ as estimated for potassium by KW (1982), is illustrated in figure 1.

Equation 2.1 represents the anisotropic limit of $\tau(\boldsymbol{K})$ without impurity scattering. Taking into account isotropic electron–impurity scattering characterised by $\tau_{imp}^{-1} \equiv \alpha = \text{const}$, then the relaxation time determining the residual resistivity ρ_r is given by the equation

$$\tau_r^{-1}(K_z) = \alpha + \beta + \gamma P_2(K_z). \tag{2.2}$$

We emphasise that, in view of the complex network of dislocations present in a real metal sample, equation (2.2) can only represent a crude description for anisotropic electron–dislocation scattering. In § 3.3 we use equation (2.2) in our calculation of A_{ee} in order to facilitate the comparison with the result of KW.

2.2. *Magnetic-field-induced anisotropy*

The second anisotropy model to be considered in the calculation of A_{ee} is based on the effect of a longitudinal magnetic field applied to a noble metal (Cu, Ag, Au). The model has been used by Thummes and Kötzler (1985) to explain qualitatively their observed enhancement of A_{ee} in Cu by a high longitudinal field. The basic idea, originally suggested by Pippard (1964) in his explanation of the longitudinal magnetoresistance in Cu, is that for $\omega_c\tau \gg 1$ (ω_c = cyclotron frequency) the fast rotating necks on the FS form belts.

Within these belts $\tau(\boldsymbol{B}, \boldsymbol{K})$ tends to zero for $\omega_c\tau \to \infty$, while in the belly regions $\tau(\boldsymbol{B}, \boldsymbol{K})$ remains essentially unaltered.

The relaxation time anisotropy in the noble metals arising from a longitudinal magnetic field $\boldsymbol{B}$ in the z-direction can be obtained from the component σ_{zz} of the conductivity. After transformation from K_x, K_y, K_z to a new set of variables ε (= energy), ϕ (= phase variable, $\dot{\phi} = \omega_c$) and K_z, which are more appropriate in the case of a magnetic field, σ_{zz} can be written as (Chambers 1969):

$$\sigma_{zz} = [e^2/(4\pi^3\hbar^2\omega_c)] \int \mathrm{d}K_z \int_0^{2\pi} \mathrm{d}\phi \times \int_0^{\infty} \mathrm{d}\phi'\, m v_z(K_z, \phi) v_z(K_z, \phi - \phi') p(\phi - \phi', \phi) \tag{2.3}$$

where $p(\phi_1, \phi_2)$ represents the probability of an electron to move in a cyclotron orbit from ϕ_1 to ϕ_2 without being scattered. For an isotropic relaxation time τ at $B = 0$ this probability is given by

$$p(\phi_1, \phi_2) = \exp[-(\phi_2 - \phi_1/\omega_c\tau)]. \tag{2.4}$$

In the following we shall assume τ at $B = 0$ to be isotropic, since here we shall only calculate the effect of the FS geometry on the relaxation time in a magnetic field. Assuming closed orbits the velocity component $v_z(K_z, \phi)$ can be expanded into a Fourier series,

$$v_z(K_z, \phi) = v_F \sum_{\nu=-\infty}^{\infty} a_\nu(K_z)\, \mathrm{e}^{\mathrm{i}\nu\phi} \tag{2.5}$$

where $a_{-\nu} = a_\nu^*$ and $v_F = \hbar K_F/m$ is the Fermi velocity on a spherical FS. By substituting this in equation (2.3) we get the following equation, first obtained by Pippard (1964),

$$\sigma_{zz} = \sigma(B = 0) \int \mathrm{d}K_z (\sigma(B)/\sigma(0))_{K_z}$$

where

$$(\sigma(B)/\sigma(0))_{K_z} = \sum_{\nu=-\infty}^{\infty} \frac{|a_\nu|^2}{1 + (\nu\omega_c\tau)^2} \left(\sum_{-\infty}^{\infty} |a_\nu|^2\right)^{-1} \tag{2.6}$$

and

$$\sigma(0) = (m/2)\,(ev_F/\pi\hbar)^2 \int \tau \sum_{-\infty}^{\infty} |a_\nu|^2\, \mathrm{d}K_z.$$

Restricting the calculation to the main symmetry directions ⟨111⟩, ⟨100⟩, and ⟨110⟩, and further assuming that the necks form sharp regions on the FS, i.e., $v_z(K_z, \phi)$ on orbits in the neck regions changes between $\pm v_0(K_z)$, one has $|a_\nu|^2 \simeq \nu^{-2}$ for odd numbers of ν and otherwise $|a_\nu|^2 = 0$. Then equation (2.6) reduces to

$$\left(\frac{\sigma(B)}{\sigma(0)}\right)_{K_z} = 1 - \frac{2N\omega_c\tau}{\pi} \tanh\left(\frac{\pi}{2N\omega_c\tau}\right). \tag{2.7}$$

Here N is the number of necks on the orbit where v_z changes sign. With the relation $(\sigma(B)/\sigma(0))_{K_z} = (\tau(B)/\tau)_{K_z}$, equation (2.7) immediately leads to the anisotropic relaxation time in a magnetic field B,

$$\tau(B, K_z) = \tau \frac{\tau(\infty, K_z)/\tau + \chi_B}{1 + \chi_B} \tag{2.8}$$

where

$$\chi_B \equiv \left[\frac{2N\omega_c\tau}{\pi}\tanh\left(\frac{\pi}{2N\omega_c\tau}\right)\right]^{-1} - 1 \tag{2.8a}$$

and

$$\tau(\infty, K_z) \equiv \begin{cases} 0 & \text{in the neck regions} \\ \tau & \text{elsewhere.} \end{cases} \tag{2.9}$$

The relaxation time $\tau(\infty, K_z)$ represents the anisotropic limit in a strong magnetic field, $\omega_c\tau \to \infty$. Figure 1 shows $\tau(\infty, K_z)$ according to equation (2.9) for the case of Cu with $\boldsymbol{B}$ parallel to the ⟨111⟩ direction. This case corresponds to the experimental situation in which the enhancement of A_{ee} has been measured and, therefore, it will be of particular interest for our calculations of the field dependence of A_{ee} in § 3.3.

3. Calculations of A_{ee}

3.1. 'Generalised' relaxation time approximation

In this subsection we calculate the dependence of A_{ee} on an anisotropic relaxation time $\tau(\boldsymbol{K})$ by use of the RTA which was first applied to this problem by KW (1980, 1982). First we present the essential steps in their treatment in order to show more clearly the approximations involved.

Since at low temperatures the resistivity $\rho_{ee} = A_{ee}T^2$ from EES is much smaller than the residual resistivity ρ_r, the calculation of A_{ee} can start from the known solution of the linearised Boltzmann equation. This means that in an external electric field $\boldsymbol{E}$ the stationary nonequilibrium distribution function $f(\boldsymbol{K})$ is determined by the known residual relaxation time $\tau_r(\boldsymbol{K})$ due to static lattice defects,

$$f[\boldsymbol{K}, \tau_r(\boldsymbol{K})] = \left[1 + \exp\left(\frac{\varepsilon(\boldsymbol{K}) - \varepsilon_F + e\boldsymbol{E}\cdot\boldsymbol{v}\tau_r(\boldsymbol{K})}{k_B T}\right)\right]^{-1} \tag{3.1}$$

where $\varepsilon(\boldsymbol{K})$ and ε_F are the band energy and Fermi energy, respectively. In the case of a magnetic field $\tau_r(\boldsymbol{K})$ has to be replaced by $\tau(\boldsymbol{B}, K_z)$ (equation (2.8)).

Now KW assume that the small rate of change in $f(\boldsymbol{K})$ arising from NEES can be approximated by a relaxation time ansatz,

$$\left.\frac{\partial f}{\partial t}\right|_{\text{scatt}}^{\text{NEES}} \simeq -\frac{f[\boldsymbol{K}, \tau_r(\boldsymbol{K})] - f[\boldsymbol{K}, \langle\tau_r(\boldsymbol{K})\rangle_{tr}]}{\tau_{ee}^{N}} \tag{3.2}$$

where

$$\langle \ldots \rangle_{tr} \equiv \int \frac{dS_F}{v_F}(\ldots \cdot v_z^2)\left(-\frac{df^0}{d\varepsilon}\right)d\varepsilon \Big/ \int \frac{dS_F}{v_F}v_z^2 \tag{3.2a}$$

denotes the transport average over the spherical FS, where unlike KW we have included the energy average in the definition in order to account for the strong energy dependence of EES.

The relaxation time τ_{ee}^{N} for NEES is taken to be independent of $\boldsymbol{K}$. Because of momentum conservation NEES cannot equilibrate the electron system but causes it to relax to a distribution $f[\boldsymbol{K}, \langle\tau_r(\boldsymbol{K})\rangle_{tr}]$ which is shifted by a constant excess momentum

$e\boldsymbol{E}\langle\tau_r\rangle_{tr}$ with respect to the equilibrium Fermi distribution $f^0(\boldsymbol{K})$.

Expanding $f[\boldsymbol{K}, \tau_r(\boldsymbol{K})]$ in equation (3.2) and retaining only terms linear in τ_r yields

$$\left.\frac{\partial f}{\partial t}\right|_{\text{scatt}}^{\text{NEES}} = -\left(\frac{\mathrm{d}f^0}{\mathrm{d}\varepsilon}\right)e\boldsymbol{E}\cdot\boldsymbol{v}\,\frac{\tau_r(\boldsymbol{K}) - \langle\tau_r(\boldsymbol{K})\rangle_{tr}}{\tau_{ee}^{N}}. \tag{3.3}$$

The form of equation (3.3) suggests the definition of an 'effective' relaxation time for resistive NEES where the latter only vanishes for constant τ_r. The total EES relaxation time with respect to resistivity is then given by the inverse of

$$\tau_{ee}^{-1}(\boldsymbol{K}) = (1/\tau_{ee}^{U}) + (1/\tau_{ee}^{N})\{1 - [\langle\tau_r\rangle_{tr}/\tau_r(\boldsymbol{K})]\} \tag{3.4}$$

where τ_{ee}^{U} is the relaxation time for UEES (also considered by KW to be independent of $\boldsymbol{K}$).

KW have not specified the conditions under which τ_{ee}^{N} and τ_{ee}^{U} are independent of $\boldsymbol{K}$. In Appendix 1 we describe the necessary approximations and show that then the scattering rates are given by (equations (A1.5) and (A1.10))

$$1/\tau_{ee}^{N} = (2\pi^2/3)(1 - \tilde{\Delta}/\tau_0) \tag{3.5a}$$

$$1/\tau_{ee}^{U} = (2\pi^2/3)(\Delta/\tau_0). \tag{3.5b}$$

The quantities $1/\tau_0$, Δ and $\tilde{\Delta}$ are defined in equations (A1.4), (A1.11) and (3.11), respectively. Here $(2\pi^2/3\tau_0)$ means the energy averaged EES rate and the factor Δ is the so-called 'fractional Umklapp scattering' (Lawrence and Wilkins 1973), which is a measure of the average current depletion in an EES event. At this point we make a clear distinction between Δ and the exact portion of UEES events $\tilde{\Delta}$, as is discussed in more detail below. Note that, different from our treatment, KW assume $\tilde{\Delta} = 0$.

The EES resistivity ρ_{ee} can now be obtained from the total resistivity $\rho_{tot} = \rho_{ee} + \rho_r = (m_{opt}/ne^2)\langle\tau_{tot}\rangle_{tr}^{-1}$ with $\tau_{tot}^{-1} = \tau_{ee}^{-1} + \tau_r^{-1}$ (n = number density of electrons),

$$\rho_{ee} = (m_{opt}/ne^2)[(1/\langle\tau_{tot}\rangle_{tr}) - (1/\langle\tau_r\rangle_{tr})]. \tag{3.6a}$$

Here m_{opt} is the optical mass which enters via the transport average (3.2*a*) (e.g., Lawrence and Wilkins 1973) and which equals the effective mass m in the case of a spherical FS. Inserting $\tau_{ee}^{-1}(\boldsymbol{K})$ from equation (3.4) into (3.6*a*) and proceeding with a simple calculation, again making use of the fact that $\tau_{ee}^{U}, \tau_{ee}^{N} \gg \tau_r$, one finally obtains the KW result,

$$\rho_{ee} = (m_{opt}/ne^2)[(1/\tau_{ee}^{U})(1 + R) + (1/\tau_{ee}^{N})R] \qquad (\tau_{ee}^{U} \text{ isotropic}) \tag{3.6b}$$

with the anisotropy parameter

$$R \equiv \langle\tau_r^2\rangle_{tr}/\langle\tau_r\rangle_{tr}^2 - 1. \tag{3.7}$$

The assumption of a $\boldsymbol{K}$-independent $1/\tau_{ee}^{U}$ in equation (3.4), which leads to the positive DMR for the UEES resistivity in equation (3.6*b*), cannot be justified theoretically. Lawrence and Wilkins have estimated that UEES contributions mainly originate from electrons within a distance $K \leqslant K_F V_G/\varepsilon_F$ (V_G = Fourier component of the pseudopotential) from the Bragg planes. Moreover, considering the case of magnetic field- or dislocation-induced anisotropy in Cu, where also the residual scattering rate $\tau_r^{-1}(\boldsymbol{K})$ is increased near the Bragg planes, one would rather expect equation (3.6*b*) to represent an upper limit for the effect of anisotropy on ρ_{ee}.

In order to have a clear separation between the effects from UEES and NEES, we

assume the validity of Mathiessen's rule for the UEES contribution. This means that the UEES resistivity ρ_{ee}^{U} has a constant value as for isotropic residual scattering. Then, instead of equation (3.6*b*) we have

$$\rho_{ee} = \frac{m_{opt}}{ne^2}\left(\frac{1}{\tau_{ee}^{U}} + \frac{1}{\tau_{ee}^{N}}R\right) \qquad (\rho_{ee}^{U} = \text{const.}). \tag{3.6c}$$

Inserting the relations (3.5) into (3.6*c*) gives the coefficient $A_{ee} = \rho_{ee}/T^2$ for anisotropic $\tau_r(\boldsymbol{K})$

$$A_{ee} = A_0[\Delta + R(1 - \tilde{\Delta})] \tag{3.8}$$

with

$$A_0 \equiv (2\pi^2/3)(m_{opt}/ne^2\tau_0)T^{-2}. \tag{3.8a}$$

For isotropic τ_r the approximations leading to (3.5) are exactly valid (see Appendix 1) and then with $R = 0$ one obtains

$$A_{ee}^{iso} = A_0\Delta \tag{3.9}$$

which is the original result of Lawrence and Wilkins. In the anisotropic limit the anisotropy parameter R achieves its maximum value $R = R^{ani}$ depending on the particular anisotropy model and consequently A_{ee} increases to A_{ee}^{ani}. The possible variation of A_{ee} within the limits $0 \leqslant R \leqslant R^{ani}$ may be expressed by the sample dependence SD as introduced by KW (1980, 1982)

$$SD \equiv \frac{A_{ee}^{ani} - A_{ee}^{iso}}{A_{ee}^{iso}} = R^{ani}\left(\frac{1 - \tilde{\Delta}}{\Delta}\right). \tag{3.10}$$

The meaning of Δ (A1.11) is different from that of the 'true fraction of UEES'

$$\tilde{\Delta} \equiv \langle|\boldsymbol{v}|^2 W_U\rangle/\langle|\boldsymbol{v}|^2 W\rangle \tag{3.11}$$

introduced in equations (A1.3) and (3.5*a*) ($W_U = W - W_N =$ UEES transition probability). While Δ measure the effectiveness of EES with respect to electrical transport, the quantity $\tilde{\Delta}$ measures the scattering rate for UEES. However, because UEES is effective in degrading the current, its relaxation time for transport should be of the same order as the UEES lifetime, and thus $\Delta \simeq \tilde{\Delta}$. Using an extension of equation (B1) in the work of Lawrence and Wilkins (1973) in the case where the wavevectors $\boldsymbol{K}_2$, $\boldsymbol{K}_3$ and $\boldsymbol{K}_4$ can be individually located near a Bragg plane, we have estimated the possible range of values:

$$\tfrac{1}{2}(G/2K_F)^2 < (\Delta/\tilde{\Delta}) \ll 8(G/2K_F)^2 \qquad \text{where } G \simeq 2K_F.$$

This estimate is supported by the numerical results of Black (1978) for Cu. It is evident from his table 10 that Δ and $\tilde{\Delta}$ agree within 10%. For $\Delta = \tilde{\Delta}$, equations (3.8) and (3.10) reduce to the simple relations

$$A_{ee} = A_0[\Delta + R(1 - \Delta)] \qquad (\rho_{ee}^{U} = \text{const}) \tag{3.12}$$

$$SD = R^{ani}[(1/\Delta) - 1]. \tag{3.13}$$

3.2. Variational method

Most of the above approximations, which are connected with the concept of a 'generalised' relaxation time, can be avoided by use of the variational method for the calculation

of A_{ee}. The main difficulties now lie in the numerical evaluation of the formally exact variational integrals.

At the low temperatures under consideration, as already mentioned above, EES has only a small effect on the stationary distribution function $f[(\boldsymbol{K}, \tau_r(\boldsymbol{K})]$, given by equation (3.1), which forms the solution of the Boltzmann equation. Thus, in the case of EES the variational method is reduced to the calculation of the EES resistivity, given by (e.g., Ziman 1960, Lawrence and Wilkins 1973):

$$\rho_{ee} = (\phi, P\phi)/(\phi, X)^2. \tag{3.14}$$

Here we take $\phi = (f - f^0)/(-\mathrm{d}f^0/\mathrm{d}\varepsilon) = -e\boldsymbol{v} \cdot \boldsymbol{E}\tau_r(\boldsymbol{K})$ as the trial solution of the Boltzmann equation $X = P\phi$. The Liouville and the collision term for EES are given by

$$X = e\boldsymbol{v} \cdot (\boldsymbol{E}/|\boldsymbol{E}|)(\mathrm{d}f^0/\mathrm{d}\varepsilon) \tag{3.15a}$$

and

$$P\phi = -\frac{1}{k_B T}\int W(1, 2 \rightarrow 3, 4) f_1^0 f_2^0 (1 - f_3^0)(1 - f_4^0)\{\phi_1 + \phi_2 - \phi_3 - \phi_4\}$$

$$\times \delta(\Delta\varepsilon) 2 \frac{\mathrm{d}^3 K_3}{(2\pi)^3} \frac{\mathrm{d}^3 K_4}{(2\pi)^3} \mathrm{d}^3 K_2 \tag{3.16a}$$

respectively, where the notation $\boldsymbol{K}_i \equiv i$ has been used throughout. $W(1, 2 \rightarrow 3, 4)$ denotes the transition probability for EES from states $\boldsymbol{K}_1, \boldsymbol{K}_2$ to $\boldsymbol{K}_3, \boldsymbol{K}_4$. The inner products are defined by

$$(\phi, \psi) \equiv \int \phi(\boldsymbol{K})\psi(\boldsymbol{K}) 2 \frac{\mathrm{d}^3 K}{(2\pi)^3}.$$

The integrals in equation (3.14) can be decomposed into surface and energy integrals. Making the reasonable assumption that $\tau_r(\boldsymbol{K})$ is independent of energy, the energy integration can be done in a way similar to that described in Appendix A of Lawrence and Wilkins (1973). Then we obtain the following expressions

$$(\phi, X) = (ne^2/m_{opt})\langle\tau_r\rangle_{tr} E \tag{3.15b}$$

$$(\phi, P\phi) = \frac{2\pi^2}{3} \frac{n}{m_{opt}} \frac{e^2}{\tau_0} \frac{\langle|\Delta\boldsymbol{v}\tau_r|^2 W\rangle}{4\langle|\boldsymbol{v}|^2 W\rangle} E^2 \tag{3.16b}$$

where we use the same notations as in Appendix 1 (equations (A1.4)–(A1.6)). Inserting into (3.14) yields

$$\rho_{ee} = \frac{2\pi^2}{3} \frac{m_{opt}}{ne^2\tau_0} \left(\frac{\langle|\Delta\boldsymbol{v}\tau_r|^2 W\rangle}{4\langle|\boldsymbol{v}|^2 W\rangle}\right) \langle\tau_r\rangle_{tr}^{-2}. \tag{3.17}$$

In order to calculate the effect of anisotropy on ρ_{ee} it is now convenient to split up the term in large brackets into a normal and Umklapp portion. The variation of the UEES contribution with the anisotropy of $\tau_r(\boldsymbol{K})$ is small compared to that of NEES, and difficult to calculate. Thus, with the same arguments as led to equations (3.6*c*), we assume ρ_{ee}^U to be independent of $\tau_r(\boldsymbol{K})$. Then equation (3.17) gives for the coefficient $A_{ee} = \rho_{ee}/T^2$,

$$A_{ee} = A_0\{\Delta + \Delta_N(1 - \tilde{\Delta})\} \tag{3.18}$$

where we have introduced the quantity

$$\Delta_N = \frac{\langle|\Delta\boldsymbol{v}\tau_r|^2 W_N\rangle}{4\langle|\boldsymbol{v}|^2 W_N\rangle\langle\tau_r\rangle_{tr}^2} \tag{3.19}$$

which is a measure of the effectiveness of NEES. Inspection of equation (3.8) shows that this expression is identical with (3.18) except that now the anisotropy parameter R is replaced by Δ_N.

We calculate Δ_N by using the Born approximation for the NEES transition probability W_N, which can be written as (e.g., Lawrence and Wilkins 1973):

$$W_N(1,2\rightarrow 3,4) = (2\pi/\hbar)[V^2(|\boldsymbol{K}_1-\boldsymbol{K}_3|) - \tfrac{1}{2}V(|\boldsymbol{K}_1-\boldsymbol{K}_3|)V(|\boldsymbol{K}_1-\boldsymbol{K}_4|)]\delta(\Delta\boldsymbol{K}). \tag{3.20}$$

For the screened Coulomb interaction among the electrons we take the Thomas–Fermi potential

$$V(q) = e^2/[\varepsilon_0(q^2 + K_{TF}^2)] \tag{3.21}$$

where the Thomas–Fermi screening wavenumber is given by

$$K_{TF} = \frac{3}{2\varepsilon_0}\frac{ne^2}{\varepsilon_F}. \tag{3.21a}$$

Furthermore, assuming a spherical FS with radius K_F (which implies that $m_{opt} = m$) and neglecting the exchange term in W_N both in the denominator and numerator of equation (3.19), we find

$$\Delta_N = I_1(K_{TF})/I_0(K_{TF}) \tag{3.22a}$$

where

$$I_0(K_{TF}) = \frac{k_{TF}}{2}\int_0^{2/k_{TF}} \frac{dx}{(x^2+1)^2}$$

$$= (k_{TF}/4)\tan^{-1}(2/k_{TF}) + k_{TF}^2/[2(4+k_{TF}^2)] \tag{3.22b}$$

$$I_1(K_{TF}) = \frac{3}{2\pi^3}\left[\prod_{i=1}^{4}\int d^3k_i\,\delta(\boldsymbol{k}_i^2-1)\right]\delta(\Delta\boldsymbol{k})$$

$$\times \frac{(k_{1z}\tau_1 + k_{2z}\tau_2 - k_{3z}\tau_3 - k_{4z}\tau_4)^2}{4\langle\tau_r\rangle_{tr}^2}\frac{k_{TF}^4}{(|\boldsymbol{k}_1-\boldsymbol{k}_3|^2+k_{TF}^2)^2} \tag{3.22c}$$

with the notations $\boldsymbol{k}_i \equiv \boldsymbol{K}_i/K_F$, $k_{TF} \equiv K_{TF}/K_F$ and $\tau_i \equiv \tau_r(\boldsymbol{K}_i)$.

For both anisotropy models under consideration (§ 2) the relaxation time depends only on the absolute value of K_z, which is taken to be the direction of the current, i.e., $\tau_r(\boldsymbol{K}) = \tau_r(|K_z|)$. In this case $I_1(K_{TF})$ can be considerably simplified, as follows. After transforming to cylindrical coordinates and using the substitutions

$$\boldsymbol{q}_\perp \equiv \boldsymbol{k}_{1\perp} - \boldsymbol{k}_{3\perp} \qquad \mu_2 \equiv \boldsymbol{q}_\perp\cdot\boldsymbol{k}_{2\perp}/(q_\perp k_{2\perp})$$

$$\boldsymbol{u}_\perp \equiv \boldsymbol{k}_{4\perp} - \boldsymbol{k}_{2\perp} \qquad \mu_3 \equiv \boldsymbol{q}_\perp\cdot\boldsymbol{k}_{3\perp}/(q_\perp k_{3\perp})$$

we can carry out the integration over $\boldsymbol{u}_\perp$, μ_2, μ_3, $\boldsymbol{k}_{2\perp}$ and $\boldsymbol{k}_{3\perp}$. Then, the only remaining δ-function is $\delta(\Delta k_z)$. Now, we make use of the fact that the integral is independent of the direction of $\boldsymbol{q}_\perp$ and substitute

$$y \equiv \frac{k_{1z}-k_{3z}}{|\boldsymbol{k}_1-\boldsymbol{k}_3|} \qquad v \equiv \frac{k_{4z}-k_{2z}}{2}$$

$$x^2 \equiv \frac{(q_\perp/k_{TF})^2}{1-y^2} = \left(\frac{|\boldsymbol{k}_1-\boldsymbol{k}_3|}{k_{TF}}\right)^2$$

$$z_2 \equiv \frac{k_{2z} + v}{a} \qquad z_3 \equiv \frac{k_{3z} + \tilde{x}y}{a}$$

with $a^2 \equiv (1 - \tilde{x}^2)(1 - y^2)$; $\tilde{x} \equiv x(k_{TF}/2)$.

Then, the last δ-function is eliminated by integration over v. The remaining integral is only threefold:

$$I_1(K_{TF}) = \frac{k_{TF}}{2} \int_0^{2/k_{TF}} \frac{F(xk_{TF}/2)}{(x^2+1)^2}\,dx \tag{3.23}$$

where

$$F(\tilde{x}) = \frac{3}{2\pi^2} \int_0^1 dy \left[\pi \int_{-1}^1 \frac{l^2(\tilde{x}y, az)}{(1-z^2)^{1/2}}\,dz - \left(\int_{-1}^1 \frac{l(\tilde{x}y, az)}{(1-z^2)^{1/2}}\,dz \right)^2 \right] \tag{3.24a}$$

$$l(x_1, x_2) \equiv (x_1 + x_2) \frac{\tau_r(x_1 + x_2)}{\langle \tau_r \rangle_{tr}} + (x_1 - x_2) \frac{\tau_r(x_1 - x_2)}{\langle \tau_r \rangle_{tr}}.$$

Here $F(\tilde{x})$ represents a weighting function for all NEES events with momentum transfer $2\tilde{x}K_F$, the form of which depends on $\tau_r(|K_z|)$. For isotropic relaxation times it follows correctly from equation (3.24*a*) that $F(\tilde{x})$ and consequently Δ_N are identically zero. In the other limit $F(\tilde{x}) = 1$, one has $\Delta_N = 1$ and consequently $A_{ee} = A_0$ from equation (3.18) with $\Delta = \tilde{\Delta}$; then all EES events contribute to $\rho_{ee}(T)$ and the lifetime $(3/2\pi^2)\tau_0$ equals the electron–electron relaxation time.

We recall that, according to equations (3.18) and (3.8), Δ_N corresponds to the anisotropy parameter R in the RTA. This result can be derived rigorously as follows: permutation symmetry of the variables permits the replacement

$$(k_{1z}\tau_1 + k_{2z}\tau_2 - k_{3z}\tau_3 - k_{4z}\tau_4)^2 \rightarrow 4k_{1z}\tau_1(k_{1z}\tau_1 + k_{2z}\tau_2 - k_{3z}\tau_3 - k_{4z}\tau_4)$$

in the integrand of (3.22*c*). Now, as discussed in Appendix 1, the basic assumption in the RTA is that in equation (A1.2) the term in braces equals unity. For a spherical FS this means that $k_{1z}\tau_1 + k_{2z}\tau_2 - k_{3z}\tau_3 - k_{4z}\tau_4$ is replaced by $k_{1z}(\tau_1 - \langle \tau_r \rangle_{tr})$. By use of these replacements in equation (3.22*c*) an elementary calculation yields a constant weighting function

$$F(\tilde{x}) = \frac{\langle \tau_r^2 \rangle_{tr} - \langle \tau_r \rangle_{tr}^2}{\langle \tau_r \rangle_{tr}^2} \equiv R \text{ for RTA} \tag{3.24b}$$

which, inserted into (3.22*a*), immediately results in $\Delta_N = R$.

3.3. Application to anisotropy models and results

Using the relations from the preceding subsections we shall now calculate the variation of A_{ee} with anisotropy in $\tau_r(\boldsymbol{K})$ for the anisotropy models from § 2.

For the simple model of dislocation-induced anisotropy in K, given by equation (2.2), there is no theoretical basis for the magnitude of the ratio γ/β. Thus, in order to facilitate the comparison with the results of KW, we adopt the value $\gamma/\beta = (7/8)^{1/2}$ assumed by KW to match the experimentally observed sample dependence.

In contrast, for our model of magnetic-field-induced anisotropy in Cu, the anisotropy of $\tau(\boldsymbol{B}, K_z)$ according to equation (2.8) is well defined by the known FS geometry of Cu (Halse 1969). The parameters determining $\tau(\boldsymbol{B}, K_z)$ are the average angular position $\bar{\vartheta}$ of the necks with respect to the field direction, the angular width $2D$ of the neck region,

Table 1. Fermi surface parameters for Cu as used in the calculation of the magnetic-field-induced anisotropic relaxation time $\tau(B, K_z)$ (equation (2.8)) and of the transport average in the anisotropic limit.

Field direction	$\bar{\vartheta}$ (deg)	D (deg)	N	$\langle\tau(\infty, K_z)\rangle_{tr}/\tau_r$
⟨111⟩	70.5	10	3	0.885
⟨100⟩	54.7	10	4	0.719
⟨110⟩	35.3	10	2	0.609

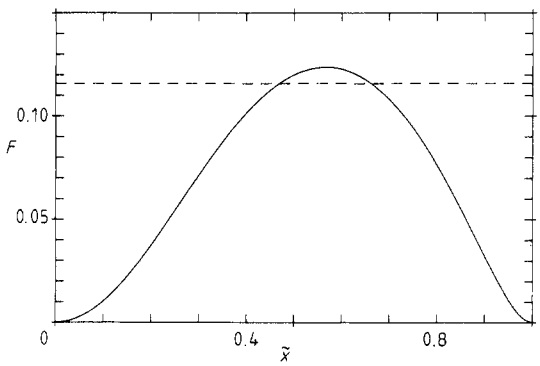

Figure 2. Anisotropic limit of the weighting function $F(\tilde{x})$ for the model of dislocation-induced anisotropy (equation (2.1)). Full curve: variational method (equation (3.24*a*)); broken curve: RTA (equation (3.24*b*)); $\tilde{x}$ measures the momentum transfer ($= 2K_F\tilde{x}$).

and the number of necks N that form a belt on the FS in which $\tau(\infty, K_z) = 0$. The appropriate values for the main symmetry directions are listed in table 1. The evaluation of $I_1(K_{TF})$ (equation (3.23)) and the weighting function $F(\tilde{x})$ (equation (3.24*a*)), which determine the parameter Δ_N (equation (3.22)), can be done by use of the Gaussian–Tschebyscheff quadrature formulae for the z-integration and Gaussian quadrature for the two other integrations. However, because of the discontinuity of $\tau(\boldsymbol{B}, K_z)$, we find it suitable to carry out the z-integration analytically as described in Appendix 2.

For the normalised screening wavenumber $k_{TF} = K_{TF}/K_F$ we use the free-electron values of 1.797 for K and 1.33 for Cu calculated from equation (3.21*a*) and $K_F = (3\pi^2 n)^{1/3}$. The resultant weighting functions in the anisotropic limit for both models, i.e, for $\alpha/\beta \to 0$ and $B \to \infty$, are shown in figures 2 and 3. The dashed lines represent the constant values of $F(\tilde{x}) = R^{ani}$ in the RTA which are obtained from (3.24*b*) in the anisotropic limit. The values of parameters Δ_N^{ani}, calculated from equations (3.22–3.24*a*) in the anisotropic limit, and R^{ani} are listed in table 2. The maximum possible variation of A_{ee} is given by the sample dependence SD defined in equation (3.10). (We retain the denotation 'sample dependence' also for the case of a magnetic field, although SD then represents the magnitude of the field dependence of A_{ee} for a particular sample orientation.) SD, given in table 2, is calculated in the approximation $\Delta = \tilde{\Delta}$ from equation (3.13) where again it is clear from (3.18) that the variational result is obtained by substituting Δ_N^{ani} for R^{ani}. For the 'fractional Umklapp scattering' Δ we have taken the calculated value of $\Delta = 0.021$ for K (MacDonald *et al* 1981) and $\Delta = 0.28$ for Cu deduced from the work of Black (1978), as discussed in more detail below.

The next interesting result from our calculations with respect to the comparison of

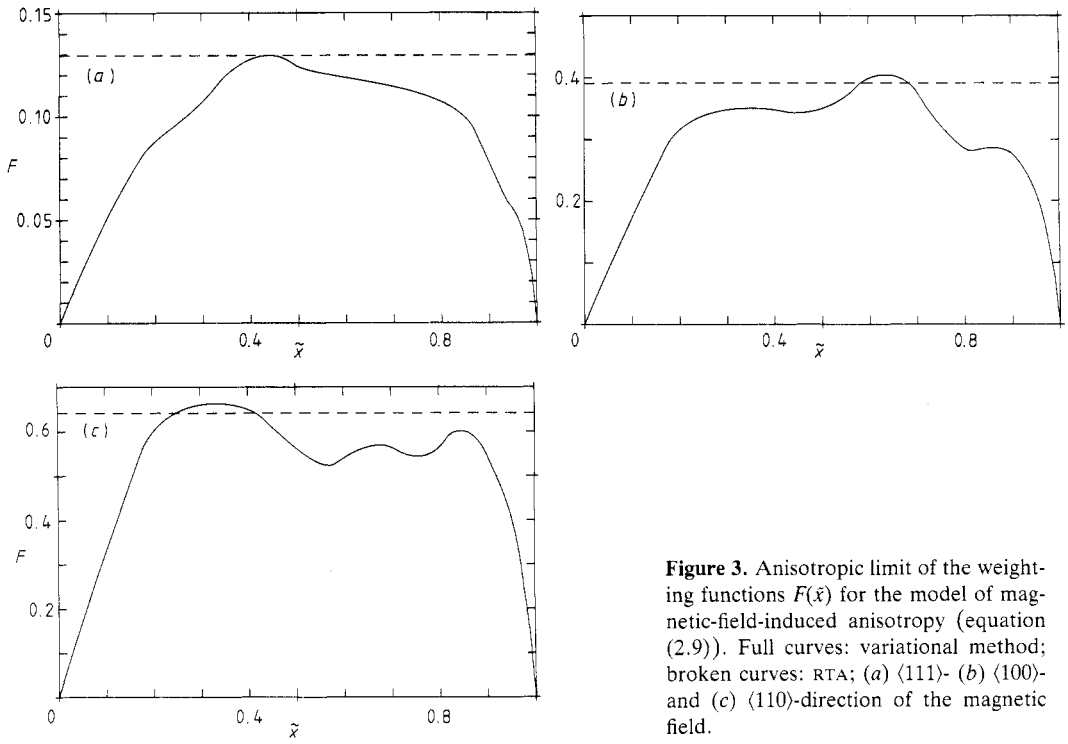

Figure 3. Anisotropic limit of the weighting functions $F(\tilde{x})$ for the model of magnetic-field-induced anisotropy (equation (2.9)). Full curves: variational method; broken curves: RTA; (*a*) ⟨111⟩- (*b*) ⟨100⟩- and (*c*) ⟨110⟩-direction of the magnetic field.

Table 2. Calculated parameters R^{ani} (equation (3.7)) (RTA) and Δ_N^{ani} (equation (3.19)) (variational method) for dislocation-induced anisotropy in K and magnetic-field-induced anisotropy in Cu and the resulting SD values for A_{ee}. The results for K are based on the assumed value of $(\gamma/\beta)^2 = \frac{2}{9}$. The experimental values of SD(exp) are discussed in § 4.

Model	R^{ani}	Δ_N^{ani}	Δ	$SD(R^{\text{ani}})$	$SD(\Delta_N^{\text{ani}})$	SD(exp)
Dislocations (K)	0.116	0.063	0.021	5.49	2.98	7 . . . 13
Magnetic field (Cu)						
⟨111⟩	0.130	0.086	0.28	0.33	0.22	≃3
⟨100⟩	0.391	0.272	0.28	1.01	0.70	—
⟨110⟩	0.642	0.488	0.28	1.65	1.25	—

the two methods and the experimental work concerns the variations of A_{ee} as a function of the variables that determine the anisotropy of the residual scattering. These variables are α/β for the case of dislocations (equation (2.2)) and $N\omega_c\tau \simeq B$ for the case of a magnetic field (equation (2.8)). We plot the variations in the normalised forms

$$(A_{ee} - A_{ee}^{\text{iso}})/(A_{ee}^{\text{ani}} - A_{ee}^{\text{iso}}) = R/R^{\text{ani}} \qquad \text{RTA} \tag{3.25a}$$

$$= \Delta_N/\Delta_N^{\text{ani}} \qquad \text{(variational method)} \tag{3.25b}$$

which follow from equations (3.8) and (3.18), respectively. These forms have the advantage of being independent of the value of Δ and $\tilde{\Delta}$. They also hold when the KW result (3.6*b*) is used.

Figure 4 shows the variation calculated from equation (3.25) for the case of dislocation-induced anisotropy. It is evident from this figure that the curves from the RTA (dashed curve) and from the variational method (full curve), both calculated for

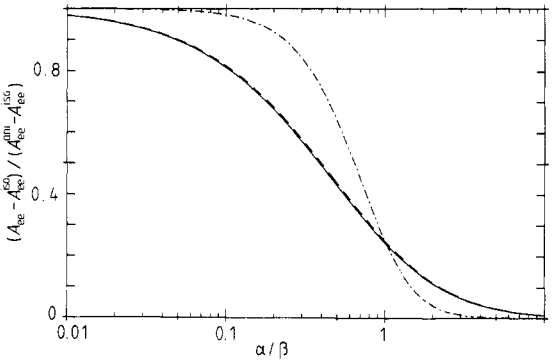

Figure 4. Normalised variation of A_{ee}, equation (3.25), as a function of α/β for the model of anisotropic dislocation scattering in K. The full curve represents Δ_N/Δ_N^{ani} and the dashed line R/R^{ani} both calculated for $(\gamma/\beta)^2 = \frac{7}{8}$. The chain curve illustrates the approximate variation for $\gamma/\beta \to 0$ according to equation (3.26), as given by Kaveh

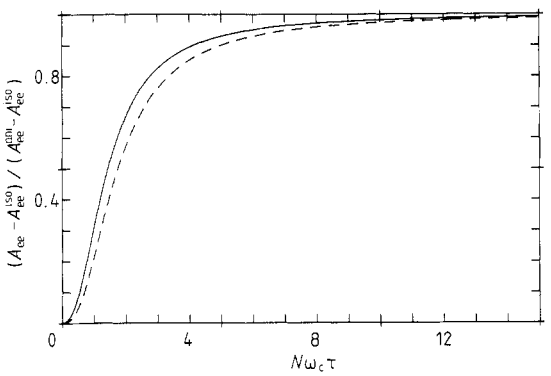

Figure 5. Normalised variation of A_{ee}, equation (3.27), as a function of $N\omega_c\tau \sim B$ in the case of a longitudinal magnetic field in Cu. Full curve: $\boldsymbol{B} \parallel \langle 111 \rangle$; dashed line: $\boldsymbol{B} \parallel \langle 110 \rangle$.

$(\gamma/\beta)^2 = \frac{7}{8}$, are nearly the same. We have also plotted the approximate expression (chain curve):

$$R/R^{ani} \simeq (1 + \alpha/\beta)^{-2} \tag{3.26}$$

given by KW (1982), which is exactly valid in the limiting case $\gamma/\beta \to 0$. On the basis of equation (3.26) KW have derived (1.1). This is easily seen by noting that $\alpha \equiv \tau_{imp}^{-1} \sim \rho_{imp}$ and approximately $\beta \sim \tau_{dis}^{-1}$, and thus $\alpha/\beta \simeq \rho_{imp}/\rho_{dis}$ which is the experimentally accessible variable entering equation (1.1). Clearly (3.26) and correspondingly (1.1) exhibit a much steeper variation around $\alpha/\beta \simeq 1$ and a faster saturation than the exact curves calculated for a more realistic value of γ/β.

In contrast to the dislocation model, the magnetic field dependence of equations (3.25) is identical for both the RTA and the variational method and is given by

$$\frac{A_{ee}(B) - A_{ee}^{iso}}{A_{ee}^{ani} - A_{ee}^{iso}} = \left(\frac{\langle \tau(\infty, K_z) \rangle_{tr}}{\langle \tau(\infty, K_z) \rangle_{tr} + \chi_B \tau} \right)^2 \tag{3.27}$$

with the values of $\langle \tau(\infty, K_z) \rangle_{tr}/\tau$ listed in table 1. Here τ is the zero-field relaxation time, assumed to be isotropic (see § 2.2), and χ_B is defined in equation (2.8*a*). In figure 5 we plot the variation of $A_{ee}(B)$, given by equation (3.27), as a function of $N\omega_c\tau$ for a $\langle 111 \rangle$- and $\langle 110 \rangle$-orientation of a sample with respect to the magnetic field. The variation for $\langle 100 \rangle$-orientation lies between these two curves and has been omitted for clarity. It is seen from figure 5 that 95% of the maximum possible increase of $A_{ee}(B)$ is already reached for $N\omega_c\tau \simeq 6$; i.e., for $\omega_c\tau \simeq 1.5$–3 when the orientation-dependent number of necks N (table 1) is taken into account. So in pure samples of Cu the saturation of the magnetic-field effect A_{ee} can already be observed at moderate fields ($\leqslant 1$ T).

4. Discussion

4.1. Comparison of RTA and variational method

As can be seen from table 2, the values of R^{ani} from the RTA are systematically higher than those of Δ_N^{ani} from the variational method, where the ratio $R^{ani}/\Delta_N^{ani} \simeq 1.3$–$1.9$ depends on the particular anisotropy model. This overestimate of the effect of an anisotropic relaxation time on A_{ee} by the RTA arises from the approximations given in Appendix 1 and its physical origin is most clearly seen from figures 1–3 as follows.

When using the RTA it is assumed that after an NEES event on the average the electrons are in $\boldsymbol{K}$-states which are characterised by an isotropic relaxation time $\langle\tau_r\rangle_{tr}$. However, this assumption cannot be justified for NEES processes with small momentum transfer $2\tilde{x}K_F$, especially in the case of a continuously varying relaxation time as $\tau_{dis}(\boldsymbol{K})$ in figure 1. It is clear from this figure that a small momentum transfer changes $\tau_{dis}(\boldsymbol{K})$ only slightly, whereas the difference from the average value $\langle\tau_{dis}\rangle_{tr}$ (corresponding to unity in figure 1) is generally large. From this it follows that for small values of $\tilde{x}$ one expects the weighting function $F(\tilde{x}) \ll R$, which is confirmed by the numerical result in figure 2. Since the relaxation time is symmetric in K_z, the same arguments hold for large momentum transfers $\tilde{x} \simeq 1$. Thus the assumption of final states with an average relaxation time is only approximately valid for an intermediate range of $\tilde{x}$ (see figure 2). This range can be considerably extended in the case of a discontinuous relaxation time anisotropy such as $\tau(\boldsymbol{B}, \boldsymbol{K})$ in figure 1, since now small momentum transfers can generate large changes in relaxation time (see figures 3*a–c*). This effect is also the reason for the finite slope of $F(\tilde{x})$ at $\tilde{x} = 0$ and 1 in these figures.

In contrast to the marked deviations in the *absolute* values of R^{ani} and Δ_N^{ani}, the *relative* changes of R and Δ_N according to equations (3.25) as a function of the anisotropy variables α/β and $N\omega_c\tau$ differ only slighly for $\tau_{dis}(\boldsymbol{K})$ (figure 4) and are identical for $\tau(\boldsymbol{B}, K_z)$ (see equation (3.27) and figure 5). This result can be understood by realising that, for an anisotropic relaxation time with a relative amplitude,

$$M \equiv \frac{\tau_r(\boldsymbol{K}) - \langle\tau_r(\boldsymbol{K})\rangle_{tr}}{\tau_r^{ani}(\boldsymbol{K}) - \langle\tau_r^{ani}\rangle_{tr}} \tag{4.1}$$

that is independent of $\boldsymbol{K}$, it immediately follows that

$$\frac{R}{R^{ani}} = \frac{\Delta_N}{\Delta_N^{ani}} = \left(\frac{\langle\tau_r^{ani}\rangle_{tr}}{\langle\tau_r\rangle_{tr}}\right)^2 M^2. \tag{4.2}$$

For $\tau(\boldsymbol{B}, K_z)$ according to equation (2.8) the amplitude $M = (1 + \chi_B)^{-1}$ is independent of K_z. Also for $\tau_{dis}(\boldsymbol{K})$ (equation (2.2)), apart from a narrow range around the pole in the denominator, M is approximately constant, thus explaining the close agreement of R/R^{ani} and Δ_N/Δ_N^{ani} in figure 4.

Our comparison of both theoretical approaches shows that the RTA may be used for an estimate of the order of magnitude of the anisotropy effect on A_{ee} and that it reproduces the relative variation of A_{ee} in cases where the form of $\tau_r(\boldsymbol{K})$ is essentially independent of the degree of anisotropy, as measured by $N\omega_c\tau$ or α/β.

4.2. Comparison with experimental work

For comparison with our theoretical results we have listed in table 2 the corresponding experimental values of *SD* for K and Cu. The data for K are taken from the review articles of KW (1984) and van Vucht *et al* (1985) and the *SD* value for Cu has been

deduced from the increase of A_{ee} in a high magnetic field observed in ⟨111⟩ Cu single crystals by Thummes and Kötzler (1985). We shall now first discuss the case of dislocation-induced anisotropy in K.

4.2.1. Potassium. Till now, in heavily strained K samples a saturation value A_{ee}^{ani} could not be detected unambiguously (van Vucht *et al* 1986). Thus the experimental SD values given in table 2 are calculated from the highest and lowest coefficients A_{ee} that have been measured in K. From the data collected by KW (1984) $SD \simeq 7$, while more recent experiments (van Vucht *et al* (1985, 1986)) yield $SD \simeq 13$. Van Vucht *et al* have pointed out that extrapolation of their data to the anisotropic limit by use of equation (1.1) may even lead to $SD \simeq 30$. However, such a high value seems doubtful because of the uncertainties involved in equation (1.1).

From a fit of $\tau_{dis}(\boldsymbol{K})$ in equation (2.1) to a sample dependence of $SD \simeq 13$ we obtain

$$(\gamma/\beta) = \begin{cases} 1.34 & \text{(RTA)} \\ 1.57 & \text{(variational method).} \end{cases}$$

These high ratios γ/β correspond to a total variation in $\tau_{dis}(\boldsymbol{K})$ by factors of 7 or 12, respectively. Such a strong anisotropy of electron–dislocation scattering appears to be unreasonable for a metal with a nearly spherical FS. However, it cannot be ruled out that a much smaller variation in $\tau_{dis}(\boldsymbol{K})$ is needed to explain the experimental SD when a different anisotropy model is used. Therefore, it is highly desirable to have a more physically established model for electron–dislocation scattering in K.

4.2.2. Copper. Before discussing the case of magnetic-field-induced anisotropy, we briefly mention that KW (1983) used the relation (2.2) also to describe for Cu the enhancement of A_{ee} by dislocations as observed upon straining Cu and *Cu*Ag samples (Steenwyck *et al* 1981, Zwart *et al* 1983). However, when using $\Delta \simeq 0.3$ from Black (1978), the measured sample dependence of $SD \simeq 3$ by Zwart *et al* cannot be explained by the anisotropy model, equation (2.1), since the necessary values of γ/β are larger than 2, and this would lead to the physically unreasonable result that $\tau_{dis}(\boldsymbol{K})$ could become negative. On the basis of the results from § 4.1 (equations (4.1) and (4.2)) we have derived a modified form of equation (1.1) for describing the effect of dislocation-induced anisotropy on A_{ee} in Cu which will be presented in a subsequent paper (Sprengel and Thummes 1989).

Now, comparison of the experimental and calculated values of SD for Cu in a longitudinal field $\boldsymbol{B} \parallel \langle 111 \rangle$ (table 2) reveals that the calculated enhancement of A_{ee} is much lower than experimentally observed. We shall consider three possible reasons for this discrepancy, two of which are connected with our theoretical model and the third with the uncertainty in the value of the 'fractional Umklapp scattering' Δ.

First, in deriving equation (3.13) for SD we have assumed the validity of Matthiessen's rule for the UEES contribution. Thus our calculated values of SD in table 2 only account for the increase in A_{ee} by NEES. If, on the other hand, we use the relation (3.6*b*) based on an isotropic UEES relaxation time τ_{ee}^{U}, we obtain for $\boldsymbol{B} \parallel \langle 111 \rangle$ and $\Delta = 0.28$:

$$\begin{aligned} SD(R^{ani}) &= R^{ani}/\Delta = 0.46 \qquad \text{(isotropic } \tau_{ee}^{U}\text{)} \\ SD(\Delta^{ani}) &= \Delta_N^{ani}/\Delta = 0.31. \end{aligned} \tag{4.3}$$

As mentioned in § 3.1 these values represent an upper limit for the contribution of UEES in the anisotropic limit and thus alone cannot explain the large differences between the

Table 3. Values of the transport average $\langle\tau(\infty, K_z)\rangle_{tr}^{c}$ and SD^{c}, calculated by use of the FS model in figure A1 and normalised to the corresponding results for a spherical FS from tables 1 and 2, respectively.

Field direction	N_s	I_s	$\dfrac{\langle\tau(\infty, K_z)\rangle_{tr}^{c}}{\langle\tau(\infty, K_z)\rangle_{tr}}$	SD^{c}/SD
⟨111⟩	0.750	0.124[a]	0.943[a]	1.53[a]
		0.115	0.957	1.39
⟨110⟩	1.002	0.391	1.001	1.00

[a] Exact integration of I_s.

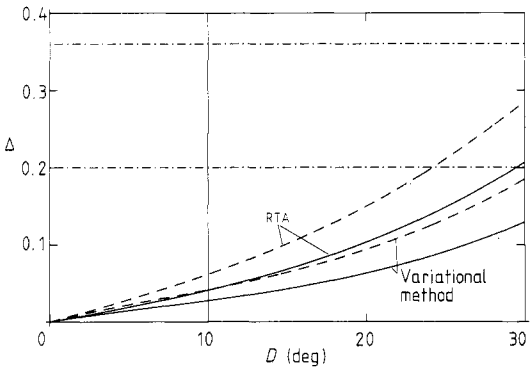

Figure 6. Values of the 'fractional Umklapp scattering' Δ as a function of the half angular width D of the neck regions that are needed to explain the experimental value of $SD = 3$ for ⟨111⟩ Cu samples in a magnetic field. Full curves: spherical FS averages; broken curves: averaging done with the FS model from Appendix 3.

theoretical and experimental result.

Second, in our theoretical approach all FS averages are calculated under the assumption of a spherical FS. In Cu the actual FS averages may be markedly different as can already be seen from the rather high value of the optical mass $m_{opt}/m \simeq 1.42$–1.54 (see table II in Beach and Christy 1977). In order to have a rough estimate of the necessary corrections for non-sphericity we consider in Appendix 3 a model FS for Cu bounded by two parallel Bragg planes. The resulting necks are either aligned parallel to the longitudinal magnetic field ($\boldsymbol{B} \parallel \langle 111\rangle$) or perpendicular to it ($\boldsymbol{B} \parallel \langle 110\rangle$); see figure A1 in Appendix 3. The calculated transport averages $\langle\tau(\infty, K_z)\rangle_{tr}/\tau$ and the corresponding SD values within RTA are listed in table 3. It is seen that for $\boldsymbol{B} \parallel \langle 111\rangle$ the additional necks give rise to an increase of SD by a factor of ~1.5, whereas for $\boldsymbol{B} \parallel \langle 110\rangle$ SD remains essentially unaltered. This demonstrates that a more realistic FS model indeed brings the theoretical value for $\boldsymbol{B} \parallel \langle 111\rangle$ closer to the experimental result but still cannot account quantitatively for the measured $SD \simeq 3$.

The third, and we believe most relevant, origin for the low theoretical SD value could consist in the uncertainty in the 'fractional Umklapp scattering' Δ for Cu calculated by Black (1978). If we use the experimental $SD \simeq 3$ and the calculated R^{ani} or Δ_N^{ani} for $\boldsymbol{B} \parallel \langle 111\rangle$, then a new value of Δ can be obtained from equation (3.13). To illustrate the possible range of Δ-values that are consistent with $SD = 3$, we have plotted in figure 6 Δ versus the half-angular width D of the neck regions. This functional dependence of Δ

on D is of interest since, experimentally, a small misalignment of the ⟨111⟩ Cu samples in the magnetic field results in enlarged effective neck regions, i.e., $D > 10°$ (see also table 1). If we make allowance for a maximum disorientation of 5° in the experiments of Thummes and Kötzler, we get $10° \leqslant D \leqslant 14°$ which, according to figure 6, corresponds to $0.03 \leqslant \Delta \leqslant 0.04$ when the variational result is used, or $0.04 \leqslant \Delta \leqslant 0.06$ from the RTA result. When the results from Appendix 3 are used (dashed curves in figure 6), the corresponding ranges are $0.04 \leqslant \Delta \leqslant 0.06$ and $0.06 \leqslant \Delta \leqslant 0.09$. These values of Δ are about a factor of five lower than the result of Black (range within the chain lines in figure 6).

There are now several indications that Black's calculations may overestimate Δ.

(i) The calculations of Δ make use of the eight-cone model of Ziman (1961) for the FS of Cu, which is not based on band structure calculations but simply has been matched to the width of the necks assumed to be circular. The corresponding pseudopotential, i.e., one half of the band gap in ⟨111⟩-direction, is $V_G = 3.5$ eV (Ziman 1961), which is much higher than the calculated and experimental value $V_G \simeq 2.4$ eV (Jepsen *et al* 1981). From the analytical approach of Lawrence and Wilkins (1973) it follows that for the noble metals $\Delta \simeq V_G/\varepsilon_F$. Thus the eight-cone model will yield a too high value of Δ. Furthermore, Black calculated Δ using two orthogonalised plane waves. MacDonald *et al* (1981) have shown that, at least in the alkali metals, the inclusion of more than two plane waves leads to a reduction of Δ by a factor of ~3, because of interference effects.

(ii) On the basis of $\Delta = 0.28$ from Black and of a theoretical value for the basic scattering rate $1/\tau_0$ for EES from equation (A1.4), the coefficient A_{ee}^{iso} can be calculated from equations (3.8*a*) and (3.9). Calculations of the basic scattering rate $1/\tau_0$ for Cu, using the Born approximation and simple Thomas–Fermi screening, give $(1/\tau_0)T^{-2} = 0.35 \times 10^6\ s^{-1}\ K^{-2}$ (Lawrence 1976, Kukkonen and Smith 1973), while the more recent calculations of MacDonald (1980), taking also into account phonon-exchange scattering, yield a value of $(1/\tau_0)T^{-2} \simeq 0.9 \times 10^6\ s^{-1}\ K^{-2}$. The corresponding EES coefficients for Cu are $A_{ee}^{iso} = 40\ f\Omega\ cm\ K^{-2}$ and $97\ f\Omega\ cm\ K^{-2}$, respectively. These coefficients are higher than the experimental value of $A_{ee} \simeq 27\ f\Omega\ cm\ K^{-2}$ for pure undeformed Cu (Steenwyk *et al* 1981, Thummes and Kötzler 1985), thus giving further evidence for the value $\Delta \simeq 0.28$ of Black being too high. On the other hand, when using the (we believe) most accurate theoretical result of MacDonald (1980), the measured $A_{ee} \simeq 27\ f\Omega\ cm\ K^{-2}$ gives Δ as low as 0.077, which is close to our deduced range of $0.04 \leqslant \Delta \leqslant 0.06$ from the variational method and Appendix 3.

Experimentally, values of Δ are obtained as follows. As has been shown by MacDonald and Laubitz (1980) the high-temperature ($T \gg$ Debye temperature) coefficient A_{ee} may be written as $A_{ee} = 5X_{ee}\Delta/(8 - 2\Delta)$. The quantity X_{ee} may be determined from the deviation from the Wiedemann–Franz law at high temperatures. For the noble metals X_{ee} has been measured by Laubitz (1970). His result for Cu is $X_{ee} \simeq 110\ f\Omega\ cm\ K^{-2}$ (±50%). Identifying the low-temperature coefficient $A_{ee} \simeq 27\ f\Omega\ cm\ K^{-2}$ with A_{ee} at high temperatures, which should be valid in Cu (MacDonald 1980), then $\Delta \simeq 0.36 \pm 0.12$, in disagreement with our suggestion. Very recently, by means of radio-frequency size-effect measurements Stubi *et al* (1988) succeeded in measuring for Cu the energy averaged EES rate $2\pi^2/3\tau_0 \simeq (2.2 \pm 0.2) \times 10^6\ s^{-1}\ K^{-2}\ T^2$ corresponding to $(1/\tau_0)T^{-2} \simeq 0.33 \times 10^6\ s^{-1}\ K^{-2}$, which is quite close to the theoretical result of Lawrence given above. Taken together with the measured coefficient A_{ee}, these experiments, for the first time, make it possible to determine Δ without any additional theoretical parameters. Identifying again the measured $A_{ee} \simeq 27\ f\Omega\ cm\ K^{-2}$ with the coefficient in the isotropic

limit, we obtain $\Delta \simeq 0.18$, which is lower than Black's value. But, as seen from figure 6, $\Delta \simeq 0.18$ is still too high to account quantitatively for the measured $SD \simeq 3$.

We note that recently also KW (1984, 1986) considered the effect of a magnetic field on the NEES contribution to the resistivity. The basic idea in their treatment is that, because of the orbital motion, a magnetic field tends to isotropise the electron distribution function in a plane perpendicular to the field and thus should reduce the NEES contribution in a sample with an anisotropic relaxation time $\tau_r(\boldsymbol{K})$. Though their results should be valid for metals with a closed FS, they are not applicable to metals with an open FS like Cu, where the existence of neck regions causes a magnetic-field-induced anisotropy, as we have shown in this work.

5. Conclusions

We have calculated the effect of an anisotropic relaxation time on the electron–electron scattering coefficient A_{ee} for resistivity in simple metals both by the use of the 'generalised' relaxation time approximation (RTA) and also, for the first time, by the use of the more rigorous variational method. Two anisotropy models have been considered, namely dislocation-induced anisotropy in K and magnetic-field-induced anisotropy in Cu. The conclusions from our results may be summarised as follows.

(i) As compared to the variational method, the RTA overestimates the magnitude of the effect of anisotropy on A_{ee} but describes the relative variation of A_{ee} with anisotropy rather well, particularly in cases where the form of $\tau_r(\boldsymbol{K})$ is nearly independent of the degree of anisotropy.

(ii) Comparison of the experimentally observed sample dependence SD in strained samples of K with our calculations reveals an unreasonably strong anisotropy of electron–dislocation scattering in K which might be related to the simplicity of the underlying anisotropy model.

(iii) In the case of Cu, our calculations clearly show that, owing to the FS topology, a longitudinal magnetic field enhances the electron–electron scattering resistivity, as has been experimentally observed in ⟨111⟩Cu single crystals. A quantitative explanation within the variational method of the measured increase of A_{ee} in a high magnetic field $\boldsymbol{B} \parallel \langle 111 \rangle$ requires a 'fractional Umklapp scattering' of $\Delta \simeq 0.04$ or $\Delta \simeq 0.06$ when the improved FS model from Appendix 3 is used. These numbers are significantly lower than $\Delta \simeq 0.28$ of Black (1978). By considering both the approximations in the calculations of Black and the theoretical and experimental results for the electron–electron scattering rate in Cu, we have given evidence that the Δ from Black may indeed be too high. Further measurements of A_{ee} in Cu for various magnetic fields and crystallographic orientations are needed in order to test the predictions from our calculations and will be helpful in drawing a clear conclusion as to the value of Δ.

Acknowledgments

We thank D J Hunt, Hamburg, for carefully reading a draft. This work has been financially supported in part by the Stiftung Volkswagenwerk.

Appendix 1. Relaxation time approximation for EES

In order to show the approximations involved in the 'generalised' relaxation time approximation (RTA) made by KW we consider the exact form of the collision integral

for NEES,

$$\left(\frac{\partial f}{\partial t}\right)_{\text{scatt}}^{\text{NEES}} = -\frac{1}{k_B T}\int W_N(1,2\rightarrow 3,4) f_1^0 f_2^0 (1-f_3^0)(1-f_4^0)$$
$$\times\{\phi_1+\phi_2-\phi_3-\phi_4\}\frac{d^3K_3}{(2\pi)^3}\frac{d^3K_4}{(2\pi)^3}2\,d^3K_2 \tag{A1.1}$$

where $\phi_i \equiv -eE\cdot v(K_i)\tau_r(K_i)$, and $W_N(1,2\rightarrow 3,4)$ = transition probability from states K_1, K_2 to K_3, K_4 for NEES. Inserting equation (A1.1) into (3.2) and allowing for current conservation we obtain:

$$\frac{1}{\tau_{ee}^N(K,\varepsilon)} = \int W_N(1,2\rightarrow 3,4)\frac{f_1^0}{f_1^0(1-f_1^0)} f_2^0(1-f_3^0)(1-f_4^0)$$
$$\times\left(\frac{(v_1\tau_1+v_2\tau_2-v_3\tau_3-v_4\tau_4)\cdot E}{(v_1\tau_1+v_2\langle\tau\rangle_{tr}-v_3\langle\tau\rangle_{tr}-v_4\langle\tau\rangle_{tr})\cdot E}\right)2\frac{d^3K_3}{(2\pi)^3}\frac{d^3K_4}{(2\pi)^3}d^3K_2 \tag{A1.2}$$

where $\tau_i \equiv \tau_r(K_i)$.

One approximation used by KW consists of setting the term in large brackets equal to unity. Then τ_{ee}^N depends only on energy and can easily be calculated,

$$\frac{1}{\tau_{ee}^N(\varepsilon)} = \frac{1-\tilde{\Delta}}{\tau_0}\frac{1}{2}\left[\pi^2+\left(\frac{\varepsilon-\varepsilon_F}{k_B T}\right)^2\right]. \tag{A1.3}$$

Here $1-\tilde{\Delta}$ is the fraction of NEES events (equation (3.11)) and $1/\tau_0$ is a basic scattering rate for EES (Lawrence and Wilkins 1973) given by

$$\frac{1}{\tau_0} = \frac{4}{3(2\pi)^9}\frac{m_{opt}}{n}\frac{(k_B T)^2}{\hbar^4}\langle |v|^2 W\rangle \tag{A1.4}$$

with the abbreviation:

$$\langle\mathcal{F}(\{S_i\})\rangle = \prod_{i=1}^{4}\int (dS_i/v_i)\mathcal{F}(\{S_i\})$$

and the transition probability W for all EES events.

With the reasonable assumption that the scattering from static lattice defects is independent of energy the energy average of $\tau_{ee}^N(\varepsilon)$ can be calculated. This yields the constant τ_{ee}^N entering equation (3.2),

$$\frac{1}{\tau_{ee}^N} \equiv \int \frac{1}{\tau_{ee}^N(\varepsilon)}\left(-\frac{df^0}{d\varepsilon}\right)d\varepsilon = \frac{2\pi^2}{3}\frac{1-\tilde{\Delta}}{\tau_0}. \tag{A1.5}$$

The relation for $\tau_{ee}^U(K)$ is similar to equation (A1.2) except that W_N is replaced by the transition probability W and the term in braces is modified,

$$\frac{1}{\tau_{ee}^U(K,\varepsilon)} = \int W(1,2\rightarrow 3,4)\frac{f_1^0}{f_1^0(1-f_1^0)} f_2^0(1-f_3^0)(1-f_4^0)$$
$$\times\left(\frac{(\Delta v\tau_r)\cdot E}{v_1\tau_1\cdot E}\right)2\frac{d^3K_3}{(2\pi)^3}\frac{d^3K_4}{(2\pi)^3}d^3K_2 \tag{A1.6a}$$

where $\Delta v\tau_r \equiv v_1\tau_1+v_2\tau_2-v_3\tau_3-v_4\tau_4$.

For $\tau_{ee}^{U}(\boldsymbol{K}, \varepsilon)$ to be independent of $\tau_r(\boldsymbol{K})$ one has to assume that the term in braces can be replaced by

$$\frac{(\Delta \boldsymbol{v}\tau_r)\cdot \boldsymbol{E}}{\boldsymbol{v}_1\tau_1 \cdot \boldsymbol{E}} \rightarrow \frac{\Delta \boldsymbol{v}\cdot \boldsymbol{E}}{\boldsymbol{v}_1 \cdot \boldsymbol{E}}. \tag{A1.6b}$$

Within these approximations the transport scattering rate for EES is given by

$$\frac{1}{\tau_{ee}(\boldsymbol{K}, \varepsilon)} = \frac{1}{\tau_{ee}^{U}(\boldsymbol{K}, \varepsilon)} + \frac{1}{\tau_{ee}^{N}}\left(1 - \frac{\langle \tau_r \rangle_{tr}}{\tau_r(\boldsymbol{K})}\right) \tag{A1.7}$$

which differs from equation (3.4) only by the $\boldsymbol{K}$-dependence of the UEES contribution. Inserting equation (A1.7) into (3.6*a*) and using $\tau_{ee}^{U}, \tau_{ee}^{N} \gg \tau_r$ results in

$$\rho_{ee} = \frac{m}{ne^2}\left(\left\langle \frac{\tau_r^2(\boldsymbol{K})}{\tau_{ee}^{U}(\boldsymbol{K}, \varepsilon)}\right\rangle_{tr} \frac{1}{\langle \tau_r(\boldsymbol{K})\rangle_{tr}^2} + \frac{1}{\tau_{ee}^{N}} \frac{\langle \tau_r^2\rangle_{tr} - \langle \tau_r\rangle_{tr}^2}{\langle \tau_r\rangle_{tr}^2}\right). \tag{A1.8}$$

In principle, the DMR for both the NEES and UEES contributions to ρ_{ee} can be calculated from this expression. However, because of the uncertainty in the explicit $\boldsymbol{K}$-dependence of $\tau_{ee}^{U}(\boldsymbol{K}, \varepsilon)$ the treatment of the UEES contribution in the presence of an anisotropic $\tau_r(\boldsymbol{K})$ needs further approximations. In making such an approximation one condition is that for isotropic τ_r equation (A1.8) must give the correct relation for ρ_{ee},

$$\rho_{ee}(\tau_r = \text{const}) = \rho_{ee}^{iso} = \frac{m}{ne^2}\left\langle \frac{1}{\tau_{ee}^{U}(\boldsymbol{K}, \varepsilon)}\right\rangle_{tr}. \tag{A1.9}$$

The assumption of KW at this point is that $1/\tau_{ee}^{U}(\boldsymbol{K}, \varepsilon)$ in equation (A1.8) is isotropic and can be approximated by its average value in (A1.9). For cubic symmetry this average is given by

$$\frac{1}{\tau_{ee}^{U}} \equiv \left\langle \frac{1}{\tau_{ee}^{U}(\boldsymbol{K}, \varepsilon)}\right\rangle_{tr} = \frac{\Delta}{\tau_0}\frac{1}{2}\int \left[\pi^2 + \left(\frac{\varepsilon - \varepsilon_F}{k_B T}\right)^2\right]\left(-\frac{df^0}{d\varepsilon}\right) d\varepsilon = \frac{2\pi^2}{3}\frac{\Delta}{\tau_0}. \tag{A1.10}$$

Here

$$\Delta \equiv \langle |\Delta \boldsymbol{v}|^2 W\rangle / 4\langle |\boldsymbol{v}|^2 W\rangle \qquad \text{with} \qquad \Delta \boldsymbol{v} = \boldsymbol{v}_1 + \boldsymbol{v}_2 - \boldsymbol{v}_3 - \boldsymbol{v}_4 \tag{A1.11}$$

is the (fractional Umklapp scattering) with respect to electric transport as first introduced by Lawrence and Wilkins (1973).

Appendix 2. Evaluation of $F(\vec{x})$ for a longitudinal magnetic field

Because of the discontinuity of the anisotropy model for Cu in a longitudinal magnetic field, equation (2.8), the convergence of the integrals over z in the weighting function $F(\vec{x})$, equation (3.24*a*), is rather weak. Therefore, in this case it is more favourable to perform the z-integration analytically as follows. For the function $l(x_1, x_2)$ in equation (3.24*a*) we use the following relations:

$$l(x_1, x_2) = l(x_1, -x_2) \equiv l_1(x_1, x_2) + l_1(x_1, -x_2) \tag{A2.1}$$

where

$$l_1(x_1, x_2) \equiv (x_1 + x_2)[\tau(x_1 + x_2)/\langle \tau\rangle_{tr}]$$

and

$$\left.\frac{dl}{dx_2}\right|_{az} = \left.\frac{dl_1}{dx_2}\right|_{az} - \left.\frac{dl_1}{dx_2}\right|_{-az} \tag{A2.2a}$$

which in the even z-integral can be written as

$$\left.\frac{\mathrm{d}l}{\mathrm{d}x_2}\right|_{az} = 2\left.\frac{\mathrm{d}l_1}{\mathrm{d}x_2}\right|_{az}. \tag{A2.2b}$$

Partial integration then leads to

$$F(\tilde{x}) = \frac{6}{\pi^2}\int_0^1 \mathrm{d}y\, a\Bigg[\pi\Bigg(l(\tilde{x}y, a)\int_{-1}^{+1}\left.\frac{\mathrm{d}l_1}{\mathrm{d}x_2}\right|_{az}\sin^{-1}(z)\,\mathrm{d}z - \int_{-1}^{+1} l(\tilde{x}y, az) \times \left.\frac{\mathrm{d}l_1}{\mathrm{d}x_2}\right|_{az}\sin^{-1}(z)\,\mathrm{d}z\Bigg) - \left(\int_{-1}^{+1}\left.\frac{\mathrm{d}l_1}{\mathrm{d}x_2}\right|_{az}\sin^{-1}(z)\,\mathrm{d}z\right)^2\Bigg] \tag{A2.3}$$

which is valid for any $\tau(K_z)$.

To evaluate $F(\tilde{x})$ for the particular anisotropy model from equation (2.8) we use inside the z-integrals the following equality

$$\left.\frac{\mathrm{d}l_1}{\mathrm{d}x_2}\right|_{az} = g(\tilde{x}y + az) + (\tilde{x}y + az)g'(\tilde{x}y + az). \tag{A2.4a}$$

Here

$$g(x) \equiv \theta(k_b - x)\theta(-k_a + x) + \theta(-k_a - x)\theta(k_b + x) \tag{A2.4b}$$

where θ denotes the Heaviside function and k_a, k_b are determined by thelower and upper boundaries of the neck regions (see figure 1).

Since $g'(x) \equiv \mathrm{d}g/\mathrm{d}x$ consists only of δ-functions, the remaining integrals are those with $g(x)$ in the integrand. Partial integration yields the final result

$$F(\tilde{x}) = \frac{3}{2\pi^2}4\pi\int_0^1 \mathrm{d}y\Bigg(\frac{\pi a^2}{8}[g(\tilde{x}y + a) - g(\tilde{x}y - a)]^2 + \tilde{x}y[g(\tilde{x}y + a) + g(\tilde{x}y - a)] \times [A(\tilde{x}y) - A(-\tilde{x}y)] - [B(\tilde{x}y) + B(-\tilde{x}y)] - \frac{1}{\pi}[A(\tilde{x}y) - A(-\tilde{x}y)]^2\Bigg) \tag{A2.5}$$

with the notations

$$A(x) \equiv A_1(x, k_a) - A_1(x, k_b)$$

$$B(x) \equiv B_1(x, k_a) - B_1(x, k_b)$$

$$A_1(x, k) \equiv \theta[a^2 - (k + x)^2]\left[x\sin^{-1}\left(\frac{k + x}{a}\right) + [a^2 - (k + x)^2]^{1/2}\right]$$

$$B_1(x, k) \equiv \theta[a^2 - (k + x)^2]\left\{\left[\left(\frac{x}{2} + \frac{a^2}{4}\right) + 2\left(\frac{x^2}{2} - \frac{a^2}{4}\right)g(k + 2x)\right]\sin^{-1}\left(\frac{k + x}{a}\right) + \left(\frac{k + x}{a}g(k + 2x) - \frac{k - 3x}{4}\right)[a^2 - (k + x)^2]^{1/2}\right\}.$$

Further evaluation of the integral in equation (A2.5) is done numerically.

Appendix 3. $\langle\tau(\infty, K_\parallel)\rangle_{\mathrm{tr}}$ in the presence of necks on the FS

We estimate the effect of non-sphericity of the FS of Cu on the transport average of $\tau(\infty, K_\parallel)$, where $K_\parallel$ denotes the component of $\boldsymbol{K}$ parallel to $\boldsymbol{B}$. For this purpose we

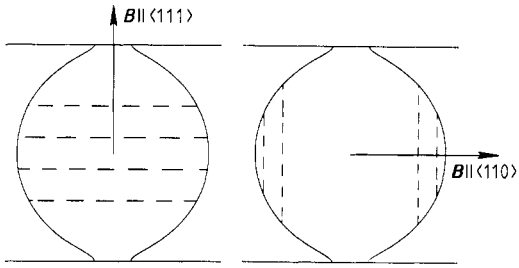

Figure A1. Fermi surface model for Cu used to estimate the effect of non-sphericity on the transport averages.

consider a model FS for Cu bounded by two parallel Bragg planes placed at $\pm G/2$ and with the magnetic field parallel to the plane normal for $\boldsymbol{B} \parallel \langle 111 \rangle$ or perpendicular to it for $\boldsymbol{B} \parallel \langle 110 \rangle$; see figure A1. The resulting necks in figure A1 do not contribute to the field dependence of $\tau(B, K_\parallel)$ and thus have been neglected in our model of magnetic-field-induced anisotropy in § 2.2. However, these necks will modify the transport averages, equation (3.2*a*).

Using two orthogonalised plane waves we get within simple perturbation theory the electron energy for the FS in figure A1,

$$\varepsilon(\boldsymbol{K}) = \varepsilon_F[k^2 + 2(g/2)(z - z_G)] = \varepsilon_F[k_x^2 + k_y^2 + (g/2)^2(\{1 + z\}^2 - 2z_G)] \tag{A3.1}$$

where $k \equiv K/K_F^c$, $g \equiv G/K_F^c$, $K_F^c \equiv (2m\varepsilon_F/\hbar^2)^{1/2}$, $z \equiv 1 - 2k_z/g$ parallel to $\langle 111 \rangle$, $z_G \equiv (\nu_G^2 + z^2)^{1/2}$ and $\nu_G \equiv (2/g)^2 V_G/2\varepsilon_F$. V_G is the pseudopotential in $\langle 111 \rangle$-direction. Using one conduction electron per atom and an angular neck radius of $D = 10°$, we calculate the Fermi energy ε_F and V_G iteratively; the results are $\varepsilon_F = 6.65$ eV and $V_G = 2.26$ eV.

The velocity of the electrons is given by

$$\boldsymbol{v}(\boldsymbol{K}) = (1/\hbar)\partial\varepsilon/\partial\boldsymbol{K} = (\hbar K_F^c/m)[k_x, k_y, (g/2)z((1/z_G) - 1)]. \tag{A3.2}$$

The surface element entering the integrals in the transport average (equation (3.2*a*)) writes now

$$\mathrm{d}S_F/\hbar v = (m/\hbar^2)\, K_F^c (g/2)\, \mathrm{d}z\, \mathrm{d}\varphi. \tag{A3.3}$$

With the notations of Appendix 2 the relaxation time $\tau(\infty, K_\parallel)$ from equation (2.9) can be written as

$$\tau(\infty, K_\parallel)/\tau = 1 - g(k_\parallel) \tag{A3.4}$$

where $g(k_\parallel)$ is defined in equation (A2.4*b*). Insertion of equations (A3.2)–(A3.4) into (3.2*a*) leads to the transport average $\langle \tau(\infty, K_\parallel) \rangle_{tr}$, which can be written in the form

$$\langle \tau(\infty, K_\parallel) \rangle_{tr}/\tau = (N_s - I_s)/N_s \tag{A3.5}$$

with

$$N_s \equiv \frac{3m}{4\pi} K_F^{-3} \int \frac{\mathrm{d}S_F}{\hbar v} v_\parallel^2 \qquad I_s \equiv \frac{3m}{4\pi} K_F^{-3} \int \frac{\mathrm{d}S_F}{\hbar v} g(k_\parallel) v_\parallel^2$$

where K_F is the free-electron Fermi wavenumber and $v_\parallel \equiv \boldsymbol{v} \cdot \boldsymbol{B}/|\boldsymbol{B}|$. The integral N_s is easily calculated analytically. For $|1 - (2/g)^2| \leqslant 2\nu_G$ the result is:

$$N_s = \left(\frac{G}{2K_F}\right)^3 \begin{cases} 1 - 3(z(z_G - z) - \nu_G^2 \ln[z_G + z] + \nu_G \tan^{-1}(z/\nu_G))_0^1 & \text{for } \boldsymbol{B} \parallel \langle 111 \rangle \\ [3(2/g)^2 - 1]/2 + \frac{3}{2}(z(z_G - z) + \nu_G^2 \ln[z_G + z])_0^1 & \text{for } \boldsymbol{B} \parallel \langle 110 \rangle. \end{cases} \tag{A3.6}$$

Further, since $g(k_\parallel)$ (equation (A2.4*b*)) is only different from zero in those regions indicated by the broken curves in figure 7, which are far from the necks under consideration, the integral I_s can be approximated by its value I_s^0 for a Fermi sphere:

$$I_s \simeq I_s^0 = k_b^3 - k_a^3. \tag{A3.7}$$

However, for $\boldsymbol{B} \parallel \langle 111 \rangle$ also an exact value for I_s can be obtained by analytical integration and subsequent iterative solution for k_a and k_b. The values of the integrals, the transport averages and the corresponding values of SD within RTA (equation (3.13)) are collected in table 3. Numbers indicated by asterisks are obtained by the exact integration of I_s.

References

Beach R T and Christy R W 1977 *Phys. Rev.* B **16** 5277
Bergmann A, Kaveh M and Wiser N 1981 *Phys. Rev.* B **24** 6807
Black J E 1978 *Can. J. Phys.* **56** 708
Callaway J 1959 *Phys. Rev.* **113** 1046
Chambers R G 1969 *The Physics of Metals Electrons* vol 1 ed. J M Ziman (Cambridge: Cambridge University Press)
Dugdale J S and Basinski Z S 1967 *Phys. Rev.* **157** 552
Halse M R 1969 *Phil. Trans. R. Soc.* A **265** 507
Jepsen O, Glötzel D and Mackintosh A R 1981 *Phys. Rev.* B **23** 2684
Kaveh M and Wiser N 1980 *J. Phys. F: Met. Phys.* **10** L37
—— 1982 *J. Phys. F: Met. Phys.* **12** 935
—— 1983 *J. Phys. F: Met. Phys.* **13** 1207
—— 1984 *Adv. Phys.* **33** 257
—— 1986 *J. Phys. F: Met. Phys.* **16** 193
Kohler M 1948 *Z. Phys.* **124** 772
Kukkonen C A and Smith H 1973 *Phys. Rev.* B **8** 4601
Laubitz M J 1970 *Phys. Rev.* B **2** 2252
Lawrence W E 1976 *Phys. Rev.* B **13** 5316
Lawrence W E and Wilkins J W 1973 *Phys. Rev.* B **7** 2317
MacDonald A H 1980 *Phys. Rev. Lett.* **44** 489
MacDonald A H and Laubitz M J 1980 *Phys. Rev.* B **21** 2638
MacDonald A H, Taylor R and Geldart D J W 1981 *Phys. Rev.* B **23** 2718
Peierls R E 1955 *The Theory of Solids* (London: Oxford University Press)
Pippard F R S 1964 *Proc. R. Soc.* A **282** 464
Schroeder P A 1982 *Physica* **109/110 B** 1901
Sprengel J and Thummes G 1989 to be published
Steenwyck S D, Rowlands J A and Schroeder P A 1981 *J. Phys. F: Met. Phys.* **11** 1623
Stubi R, Probst P-A, Huguenin R and Gasparov V A 1988 *J. Phys. F: Met. Phys.* **18** 2479
Thummes G and Kötzler J 1985 *Phys. Rev.* B **31** 2535
van Vucht R J M, van Kempen H and Wyder P 1985 *Rep. Prog. Phys.* **48** 853
van Vucht R J M, van de Walle G F A, van Kempen H and Wyder P 1986 *J. Phys. F: Met. Phys.* **16** 1525
Wiser N 1984 *Contemp. Phys.* **25** 211
Ziman J M 1960 *Electrons and Phonons* (London: Oxford University Press)
—— 1961 *Adv. Phys.* **10** 1
Zwart J, Pratt W P Jr, Schroeder P A and Caplin A D 1983 *J. Phys. F: Met. Phys.* **13** 2595